Concept of a photon-counting camera based on a diffraction-addressed Gray-code mask

Sébastien Morel

European Southern Observatory, avenida Alonso de Córdova 3107, Vitacura, Chile

ABSTRACT

A new concept of photon counting camera for fast and low-light-level imaging applications is introduced. The possible spectrum covered by this camera ranges from visible light to gamma rays, depending on the device used to transform an incoming photon into a burst of visible photons (photo-event spot) localized in an (x, y) image plane. It is actually an evolution of the existing "PAPA" (Precision Analog Photon Address) Camera that was designed for visible photons. This improvement comes from a simplified optics. The new camera transforms, by diffraction, each photo-event spot from an image intensifier or a scintillator into a cross-shaped pattern, which is projected onto a specific Gray code mask. The photo-event position is then extracted from the signal given by an array of avalanche photodiodes (or photomultiplier tubes, alternatively) downstream of the mask. After a detailed explanation of this camera concept that we have called "DIAMICON" (DIffraction Addressed Mask ICONographer), we briefly discuss about technical solutions to build such a camera.

Keywords: Photon-counting cameras, spot position encoding.

1. INTRODUCTION

Fast imaging is usually related to low-light level detection because of the short exposure time required. Detectors that are able to reach the quantum limit, by individually detecting photon positions in the image plane, are mandatory for this purpose. Although research in CCD detectors has allowed to reach the quantum limit in certain conditions,[1] such solid-state detectors remain in some case too slow to compete with micro-channel plate (MCP) based photon-counting cameras. Moreover, high-energy photon imaging remains a niche reserved for for MCP-based cameras. Among recent innovations in these devices are: the Photon Address Digital Detector System (PADDS),[2] and the DELTA Camera.[3] The PADDS employs a position-sensitive photo-multiplier and offers a low 128×128 pixel resolution with some distortion. The DELTA camera project aimed to build a 512×591 pixel camera with a 2.6 μs time resolution. It had to be aborted because it planned to feature Thomson fast readout linear CCDs that are not manufactured anymore. A lesson we can draw from this ill-fated experiment is that one should not rely too much on the availability of "exotic" commercial components.

The PAPA Camera,[4] invented in 1982, provides fast (1 μs time resolution) and high-rate (1 million photo-events/s) counting. The design of this camera is reminded by Fig.1. The PAPA can easily be built from standard off-the-shelf components and does not require high-vacuum equipment for its construction. The main inconvenient of the PAPA is the complexity of its optical system, generating artifacts that are difficult to correct.[5] We therefore propose a new design of camera (the "DIAMICON"), which could re-use most of the PAPA components, but with a single-lens design to minimize possible artifacts.

2. GENERAL CONCEPT

The DIAMICON project (Fig. 2) features a second or third generation (MCP-equipped) image intensifier. Each photon striking the photocathode of the intensifier ("photo-event") generates a light spot on the phosphor screen located at the other end of the intensifier, at the same position in the image plane. Alternatively, for high-energy photon applications, a NaI(Tl) scintillator could be used instead of the image intensifier. A large achromatic lens with short f/D re-images the spots on the plane of the Gray mask.

While the PAPA Camera re-images the phosphor screen plane as an array of small identical images by the mean of secondary lenses (while the large lens is used as a collimator), the DIAMICON re-images the phosphor

Further author information: E-mail: smorel@eso.org

screen plane as a sole image. In the pupil plane of the sole lens, a diffraction filter has been located, in order to transform each spot from the image intensifier or the scintillator into a 4-branch cross pattern. Such filters exist for art photography, and are usually made of a fine mesh etched on a plate. In our case, we need to optimize the design of the filter, such that most of the light is spread over the branches of the cross (see Sec. 4).

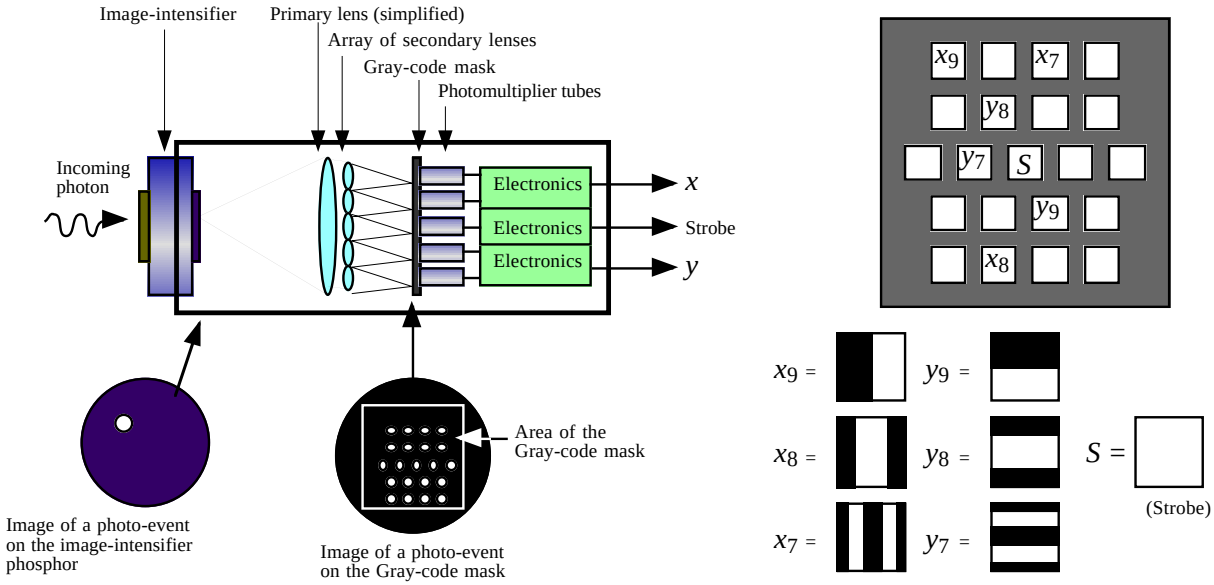

Fig. 1. The original PAPA Camera concept. The Gray-code mask is a fictive case for a 10-bit coordinate coding (1024×1024 pix.). The mask elements for the three most significant bits of x and y are shown. The strobe mask is empty and is used to valid the presence of a photo-event.

The cross pattern is projected on the Gray-code mask. This mask consists of an array of $n \times n$ square mask elements. Each mask element can block or transmit the light to one or several elementary light detectors (ELDs). An ELD is any high-sensitivity compact light sensor: it can be either a photomultiplier tube (PMT), as in the case of the PAPA Camera, or a solid-state component like an avalanche photodiode (APD) in Geiger mode. Each ELD is associated to a discriminator to convert the analog signal at the output of the component into a 1-bit binary signal.

Thus, each ELD has an associated state δ, having either the value 0 ("no light received") or 1 ("light received"). Although there are several solutions to encode the coordinates, we set as a constraint, that all the mask elements are arranged into a square array. Moreover, one mask element should correspond to one ELD, and one ELD to one mask element. This will simplify the design of the mask-to-ELD coupling. Depending on where the cross pattern is projected on the mask, the light from the cross pattern will reach some ELDs. The set of states of all the ELDs can be described as a matrix $\{\delta_{ij}\}$ $(0 \leq i < n; 0 \leq j < n)$. This state matrix can be processed by a real-time computer that yields the (x, y) coordinates of the photo-event.

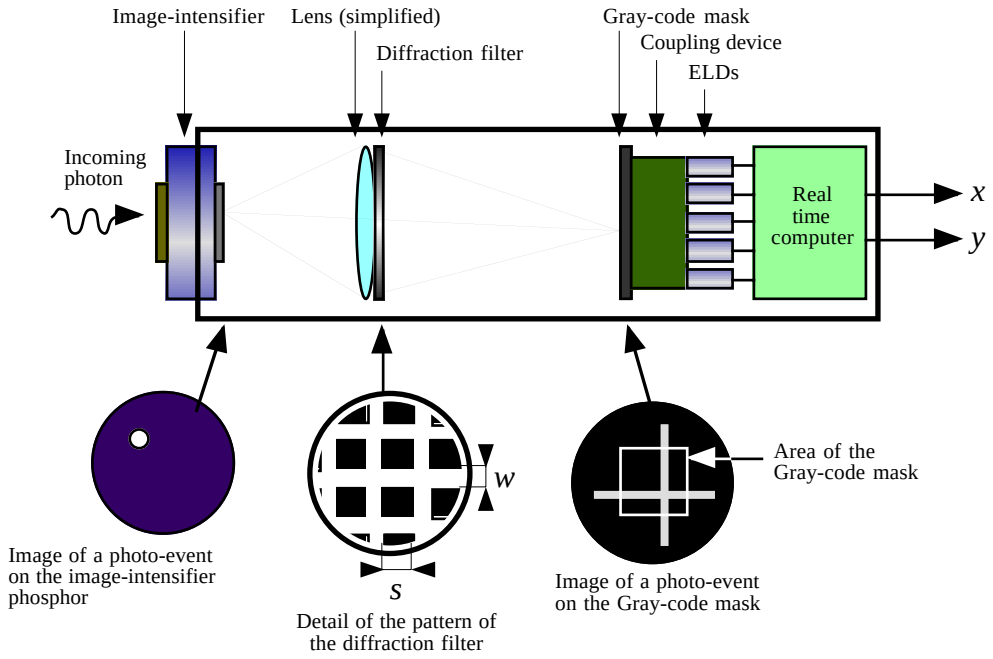

Fig. 2. Schematic of the DIAMICON Camera.

Because of the shape of the cross pattern, only one column and one row of ELDs are illuminated from a photo-event, and the coordinates are retrieved as follows (Fig. 3):

- The column (resp. the row) having at least two ELDs with $\delta = 1$, yields:

$$X_a = \text{int}\left(\frac{x}{2^{n-1}-1}\right),$$
$$\text{resp.} \quad Y_a = \text{int}\left(\frac{y}{2^{n-1}-1}\right),$$

  where 'int' is the integer part of a real number.

- The state of each ELD in this column (resp. this row) depends on whether its associated mask element blocks or transmits the light from the cross pattern. The set of the states yield the Gray coded value of:

$$X_b = 2 \times \left(x \bmod (2^{n-1}-1)\right) + 2,$$
$$\text{resp.} \quad Y_b = 2 \times \left(y \bmod (2^{n-1}-1)\right) + 2,$$

  where 'mod' is the modulus (remainder from an euclidean division).

- Hence, the retrieved coordinates are:

$$\hat{x} \quad = X_a \times (2^{n-1}-1) + \tfrac{X_b-2}{2} = x$$
$$\hat{y} \quad = Y_a \times (2^{n-1}-1) + \tfrac{Y_b-2}{2} = y$$

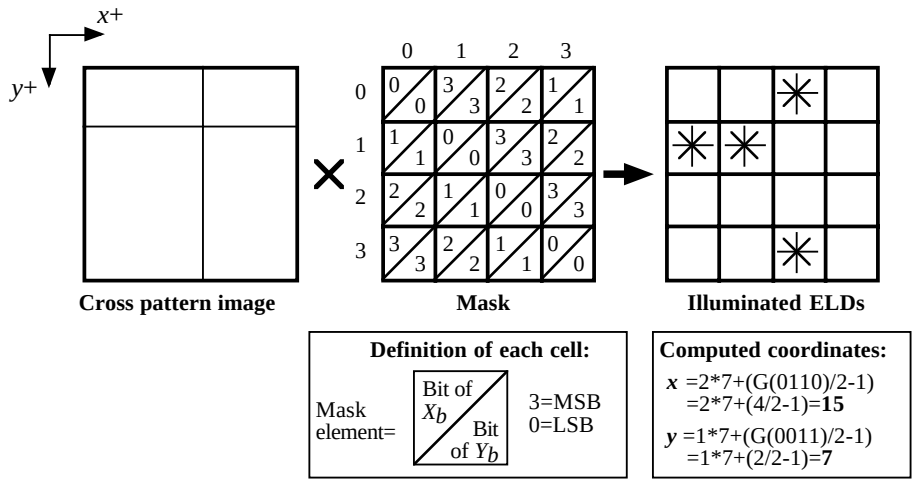

Fig. 3. How the photo-event coordinates are retrieved from the position of the cross pattern on the mask of the DIAMICON camera (if $n = 4$). The 'G' function is the transformation of a binary Gray value into its associated decimal value.

The above formulas come from two rules:

1. No Gray-code numbers with an odd number of bits at 1 are used for the fine coding (X_b, Y_b) of the coordinates
2. The zero value is not used either.

These rules are necessary to avoid the following ambiguity cases, where the solution for (x, y) from $\{\delta_{ij}\}$ is not unique (Fig. 4):

1. A column u (resp. a row v) with $\delta_{uj} = 0\ \forall j$ (resp. with $\delta_{iv} = 0\ \forall i$) cannot be seen as illuminated by the cross pattern.
2. Only one ELD with $\delta = 1$ in a column and one in a row cannot define them as illuminated by the cross pattern: let u be the illuminated column, and v the illuminated row. If $\delta_{uv'} = 1$ corresponds to the only ELD illuminated in the column u, and $\delta_{u'v}$ corresponds to the only ELD illuminated in the row, there is ambiguity case: either $(X_a, Y_a) = (u, v')$, or $(X_a, Y_a) = (u', v)$.
3. If a column (resp. a row) has only one ELD with $\delta = 1$, while a row (resp. a column) has several ELDs with $\delta = 1$, and if rule 1 (no zero value) is applied, it is not possible to determine which ELD with $\delta = 1$ corresponds to the row (resp. the column) illuminated by the cross pattern.
4. If the central peak of the cross pattern illuminates an ELD, it is not possible to know whether this ELD for which $\delta = 1$ fine codes a bit at 1 for X_b, or for Y_b, or for both. The way to eliminate this ambiguity consists in only allowing even numbers of ELD for which $\delta = 1$ in a column (resp. a row) to encode the value of X_b (resp. Y_b). In this case, if a column (resp. a row) is found with an odd number of ELDs with $\delta = 1$, the resulting encoded value of X_b (resp. Y_b) cannot be valid, and the ELD with $\delta = 1$, illuminated by the central peak and corresponding to the intersection of the illuminated row and column, belongs to the coding of Y_b (resp. X_b) given by the illuminated row (resp. column).

The resolution of a camera employing this coding system is therefore $n(2^{n-1} - 1) \times n(2^{n-1} - 1)$ pixels. One may notice that, at similar resolution, the required number of ELDs is more important than for the PAPA Camera: for $n = 5$ (25 ELDs), the resolution of the DIAMICON would only be 75×75 pixels, while a PAPA

with 21 ELDs already provides a theoretical resolution equal to 1024 × 1024 pixels ($n = 8 \Rightarrow 64$ ELDs would be required by our camera to get a 1016 × 1016-pixel resolution). This drawback is not considered as critical, thanks to the progress in electronics since 1982: the extra ELDs that are required, like PMTs with their discriminators, can be procured at low cost. The development of avalanche photodiode arrays[6] also opens an opportunity to build a DIAMICON, with a high resolution and the advantage of a solid-state integrated detector. Moreover, the progress in embedded computers allows to process in real time the data from the ELDs to convert them into (x, y) photo-event coordinates.

Using a modified Gray-code values with an even number of bits only may unfortunately lead to glitches (that the normal Gray-code is supposed to prevent from occurring), because two bits need to be changed to shift from one value to the next one. However, these glitches are identified by columns or rows with an odd number of "$\delta = 1$" states, and can then be discarded. The glitch probability depends on the "thickness" of the branches of the cross pattern compared to grid step of the lowest bit mask-element. The diffraction limit $\bar{\lambda}/D$ (where $\bar{\lambda}$ is the average wavelength of the spot emitted by the phosphor screen) of the re-imaging lens, and the size of a photo-event spot on the phosphor screen of the image intensifier, determine the branch thickness. The situation where glitches for both x and y occur at the same time may be confusing, but is not critical if this event has a low probability compared to the thermoionic emission from the photocathode of the image intensifier (causing detection of false photo-events), in case such a device is used as photo-event amplifier.

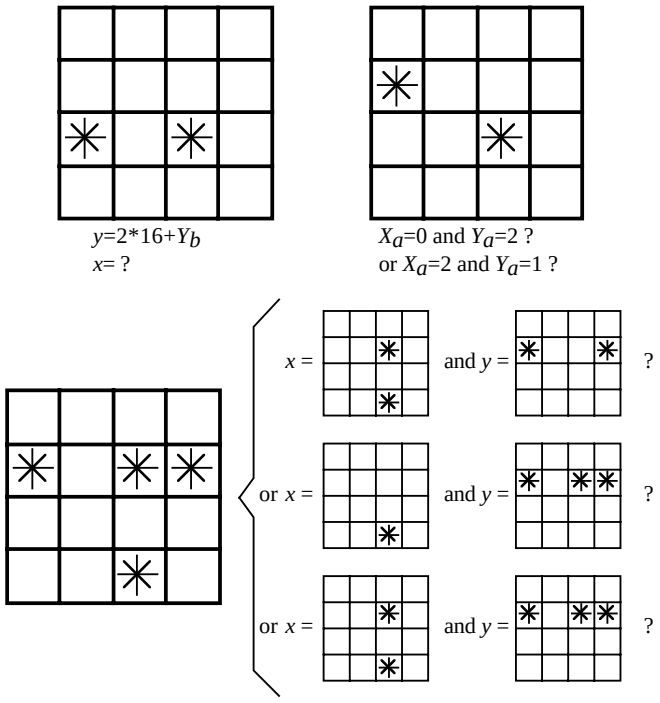

Fig. 4. Cases illustrating why restrictions have to be applied for possible Gray-code values of X_b and Y_b (if $n = 4$). Top-left: if the zero value is allowed and $X_b = 0$ x cannot obviously be determined ; Top-right: if one bit at 1 in the Gray-codes of X_b and Y_b is allowed, two possible values exist for (x, y). Bottom: if the Gray-codes of X_b and Y_b with an odd number of bits at 1 are allowed, three possible values exist for (X_b, Y_b).

3. GRAY-CODE MASK DESIGN

The design of the mask is mostly driven by the mechanical characteristics of the ELD coupling device, i.e., how the individual sensitive areas for each ELD are arranged in the plane right behind the mask.

Each cell of the $n \times n$ ELD array is associated with a square mask element giving both a Gray-code bit of the value of X_b, and a Gray-code bit of the value of Y_b. The shape of this mask element is the result of a binary "AND" between the mask element for the Gray-code bit of X_b given by the column, and the mask element for the Gray-code bit of Y_b given by the row, if we consider that an opaque region of a mask element is equivalent to 0, and a transparent zone to 1 (Fig. 5).

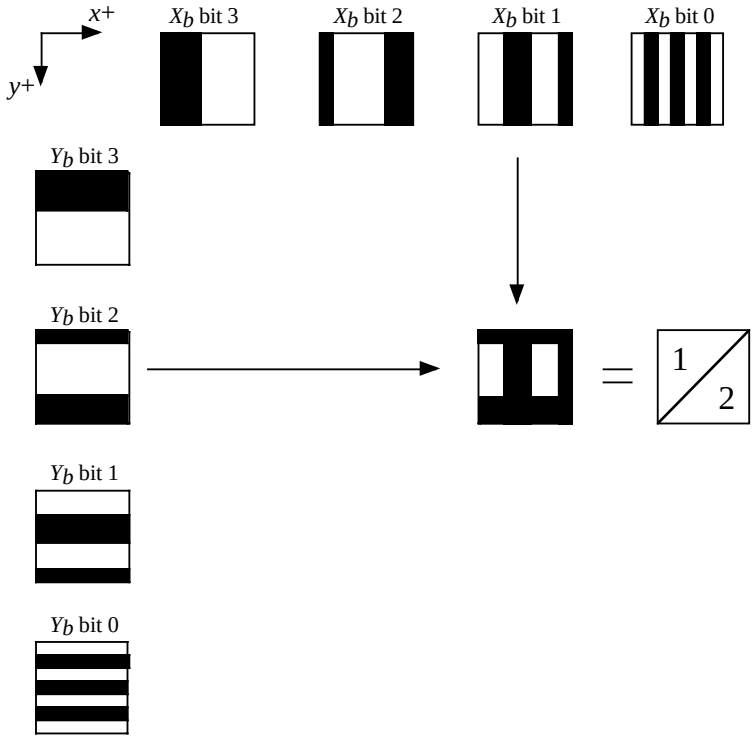

Fig. 5. Elementary masks that are used to encode X_b and Y_b ($n = 4$ case), and how a mask element is made.

It is important to notice than any mask element linked to an ELD can code any Gray-code bit of X_b and any Gray-code bit of Y_b. This flexibility allows to solve the problem of the fill factor of the coupling device behind the mask: whether we use an APD array or or a bundle of fibers linked to a set of PMTs or APDs, the sensitive area of the coupling device, located right behind the mask, is expected to have "dead zones" that cannot detect any photon from the light coming from the horizontal or the vertical branches forming the cross pattern. Therefore, all the dead zones of the sensitive area of the coupling device should correspond to the opaque region of the mask.

The dead zone constraint determines the way the Gray-code bits for X_b and Y_b are associated to each ELD. The number of possible mask designs can be estimated to be $(n!)^{2n}$. Just for $n = 4$, there are already about 1.1×10^{11} possible masks. However this figure is overestimated and does not take into account mask subsets that are equivalent after a geometrical transformation (like a rotation by 90° clockwise, or counter-clockwise) of some of them. Even in this case, the number of possible masks remains high, and for $n = 8$, it is not easy to find the right mask design. One may use genetic algorithms to find it, using the minimum mechanical distance allowed between two inputs of the coupling device as a constraint.

If we use, as a coupling device, a bundle that is made of mechanically separated fibers, the constraints on the mask design are relaxed, because the fiber heads can be arranged in any position, and not only as a squared

matrix. Moreover, fibers with different diameters of feeding optics (focusing lenses) can be used. It is also relevant to notice that only a part of the light going through the mask may be tapped, provided that the resulting level of light is enough for detection by an ELD. If it is possible to feed an ELD with more than one fiber, even more flexibility is allowed. Fig. 6 shows a possible arrangement of fibers for an $n = 4$ mask.

Unlike the PAPA, for which the physical size of the mask was dictated by the aperture of the primary lens, the physical size of the DIAMICON mask depends on the desired magnification factor of the lens, determined by its distance to the phosphor screen. This may help (within reasonable limits that are fixed by the maximum physical camera size wished) to solve the problem of the mask design. Moreover, one can notice that the Hamming distance between any two non-null four-bit binary numbers with an even number of bits is always 2. Hence, other codes than the "even parity Gray" can be used to code X_b and Y_b. The possibility to use an alternative code that would ease the mask design (by relaxing again the "dead zone" constraint) should be investigated

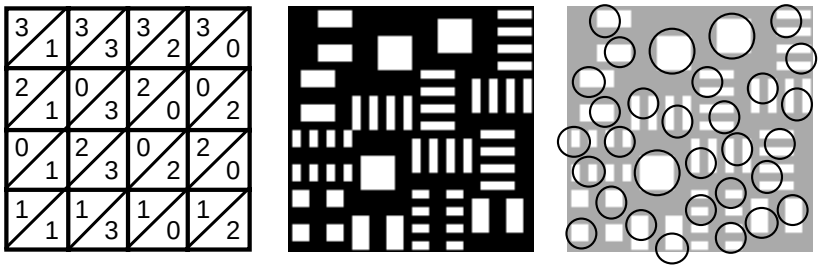

Fig. 6. Mask with $n = 4$ represented by the formalism which is used in the previous figures (left) ; the same mask that would be made by photo-etching (center) ; repartition of tapping fiber-optics (feeding ELDs) in the plane of the mask, two diameters of fiber collectors are used (right)

4. DIFFRACTION FILTER DESIGN

The design of an ideal diffraction filter for the DIAMICON camera is still pending. We just give here some hints resulting from numerical simulations.

For example, we have noticed that the energy in the central peak is reduced when a "negative mesh", (i.e. an array of opaque squares separated by transparent lines) is used as a filter (Fig. 2). The width w of the transparent lines of the filter determines the angular size of the branches: each branch will have an efficient angular size of $\bar{\lambda}/(2w)$. The branches should be large enough to span over the mask for the internal field-of-view of the camera (corresponding to the solid angle of the phosphor screen as seen by the re-imaging lens). In this case, w would likely need to be less than 10 μm. The final optical design of the camera will determine the exact value for w. Concretely, the filter can be made, like the mask, by high-precision photo-etching on a glass plate.

To spread the energy over the branches, the size s of the opaque squares must be large compared to w. The drawback is a global loss of energy within the central peak and the branches: the transmission of the filter is $1 - s^2/(s + w)^2$. There is therefore a trade-off between the allowed maximum intensity (which would not cause any artifact) and the sensitivity of each ELD. In other words, the dynamic range of the ELDs are the main constraint for the design of the filter.

We have found from numerical simulation that $s = 7w$, would probably be a good compromise: for monochromatic light, 18.3% of the energy from the output is in the central peak and the transmission of the filter is 23.4%.

Regarding the actual polychromatic case, one may notice that such a filter behaves like a grating for spectroscopy, with the presence of multiple orders. We simulated the case of a diffraction filter illuminated by a P-47 (short afterglow) phosphor: $\bar{\lambda} = 440$ nm, with FWHM=100 nm. The $s = 7w$ pattern yields 21% of the energy from the output is in the peak, and 68% is in the branches of the cross pattern. However, due to this "grating" effect, on may notice the presence of gaps (Fig. 7) in the branches at the neighborhood of the central peak.

One trick to solve this problem consists in superimposing two grids with different steps. For example, $s = 9.5w + s = 11.5w$ gives smoother branches in the cross pattern, but as a drawback compared to the "$s = 7w$" grid, 27% of energy in the central peak and 60% in the branches. Nevertheless, the "radial streaks" outside the cross (which can be noticed on the "$s = 7w$" grid on Fig. 7) tend to be smeared out. This should reduce the probability of false "$\delta = 1$" events that might be caused by such artifacts. However, improving the filter is still possible, and as for the Gray-code mask, optimization algorithms should be used in order to find out the best filter pattern.

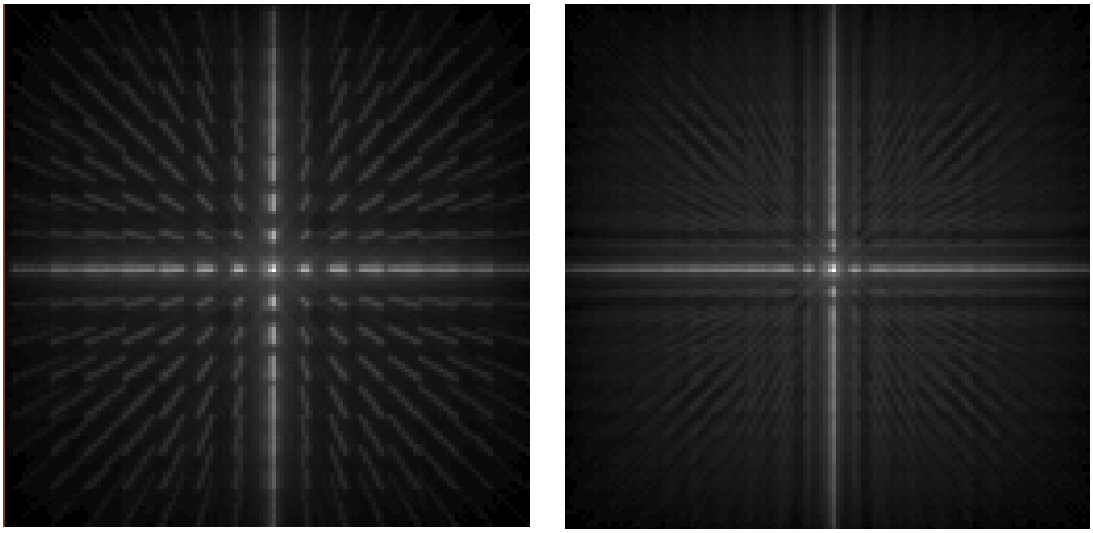

Fig. 7. Examples of cross patterns obtained by numerical simulation of diffraction filters illuminated by a P-47 phosphor. Left: $s = 7w$ case ; right: $s = 9.5w + s = 11.5w$ case. Note that due to computer limitation, the aperture of the filter had to be reduced. Actual cross patterns would be more elongated. These images have been printed after a gamma correction with $\gamma = 0.2$ to better show the existing artifacts.

5. CONCLUSION

Our aim was to present an innovative and simple concept of photon-counting camera derived from the PAPA Camera. A significant engineering work would remain to be done to get the final design of the DIAMICON camera. A 16-ELD (4×4) prototype for demonstration can easily be made from the components of any existing PAPA Camera, though an 8×8 version will probably be required for astronomical applications. It is interesting to notice that the optical set-up of the DIAMICON, used to locate photo-event spots, can also be applied to any fast spot-tracking application.

REFERENCES

1. C. D. Mackay, R. N. Tubbs, R. Bell, D. J. Burt, P. Jerram, and I. Moody, "Subelectron read noise at MHz pixel rates," in *Sensors and Camera Systems for Scientific, Industrial, and Digital Photography Applications II*, M. M. Blouke, J. Canosa, and N. Sampat, eds., *Proc. SPIE* **4306**, p. 289, 2001.
2. M. Pruksch and F. Fleischmann, "Photon address digital detector system (PADDS): a cost-effective imaging photon detector," *Appl. Opt.* **39**, p. 2443, 2000.
3. S. Morel and L. Koechlin, "The DELTA photon counting camera concept," *Astron. & Astroph. Suppl. Series* **130**, p. 395, 1998.
4. C. Papaliolios and L. Mertz, "New two-dimensional photon camera," in *Instrumentation in Astronomy IV*, *Proc. SPIE* **311**, p. 360, 1982.
5. P. R. Lawson, "Artifacts in PAPA camera images," *Appl. Opt.* **33**, p. 1146, 1994.
6. S. Vasile, P. Gothoskarl, S. Drulla, and R. Farell, "Photon detection with high gain avalanche photodiode arrays," *IEEE Trans. Nucl. Sci.* **45**, p. 720, 1998.